An integrated simulation method for coupled dynamic systems

Xu Huang[1] and Oh-Sung Kwon[2]

[1] Ph.D. Candidate, Department of Civil and Mineral Engineering, University of Toronto - Toronto, ON, Canada.
[2] Associate Professor, Department of Civil and Mineral Engineering, University of Toronto - Toronto, ON, Canada.

ABSTRACT

Partitioned analysis methods have been mostly used in multiphysics and large-scale media problems since they allow decomposition of a complex system into smaller problems. Although they have been considered to be superior to monolithic methods in terms of software reuse, difficulties still exist in the implementation process. This study addresses these difficulties and proposes a new method to ease the coupling of the substructures analyzed with different Finite Element (FE) codes. This is enabled by the development of a staggered partitioned approach such that each involved program acts as a black box which is accessible through standard model input and output, i.e. displacements and forces at the boundary of each model. In addition, the substructures can be numerically integrated using any α-modified integration scheme (explicit or implicit). A general stability proof is provided to determine the maximum time step to ensure a stable solution. An example application will be presented which demonstrates potential of the developed integrated simulation method.

Keywords: Coupled Dynamic System, Substructuring, Integration Scheme, Stability, Finite Element Method

INTRODUCTION

Integrated simulation methods, also termed as partitioned or coupled methods, are most suited for performance assessment of large structural systems as they allow conversion of a large problem into several small problems whose size and complexity can be handled by conventional simulation methods.

Considering a large system whose equation of motion can be expressed as

$$\boldsymbol{M}\boldsymbol{a} + \boldsymbol{C}\boldsymbol{v} + \boldsymbol{R} = \boldsymbol{F} \tag{1}$$

where $\boldsymbol{M}$ and $\boldsymbol{C}$ are system mass and damping matrices, $\boldsymbol{R}$ and $\boldsymbol{F}$ are restoring force and external load vectors, $\boldsymbol{a}$ and $\boldsymbol{v}$ are acceleration and velocity vectors. There are mainly two types of methods to decompose the equation. For the sake of simplicity, it is assumed that a system is decomposed into two substructures i and j which are independently modelled with analysis modules X and Y, respectively.

Method-a: decomposition is only made for the damping and/or restoring forces of the system. Then Eq. 1 can be rewritten as

$$\boldsymbol{M}\boldsymbol{a} + \boldsymbol{C}_i\boldsymbol{v}_i + \boldsymbol{C}_j\boldsymbol{v}_j + \boldsymbol{R}_i + \boldsymbol{R}_j = \boldsymbol{F} \tag{2}$$

where the subscripts i and j denote the relevant terms of substructure i and j, respectively. Figure 1(a) illustrates the way to model the substructures with analysis module X and Y. Including the inertia properties and the external load of the entire system, module X acts as the main solver of the equation of motion (Eq. 2) in addition to the computations of the damping and restoring forces for the substructure i. Module Y, on the other hand, only works as a slave to the module X and its main task is to determine the $\boldsymbol{C}_j\boldsymbol{v}_j$ and $\boldsymbol{R}_j$ and provide them to the module X. This method has been mostly used in the current hybrid simulation tests [1,2] where the module Y can be a sophisticated numerical model or a physical specimen. Since the behaviour of the critical portions is often dominated by a few structure components, this method is referred to as a component-level decomposition method.

Method-b: decomposition is not only made for damping and/or restoring forces but also for the inertial properties of the system.

$$\boldsymbol{M}_i\boldsymbol{a}_i + \boldsymbol{M}_j\boldsymbol{a}_j + \boldsymbol{C}_i\boldsymbol{v}_i + \boldsymbol{C}_j\boldsymbol{v}_j + \boldsymbol{R}_i + \boldsymbol{R}_j = \boldsymbol{F}_i + \boldsymbol{F}_j \tag{3}$$

The modelling of the two substructures with analysis modules X and Y is shown in Figure 1(b). Different from the master-slave approach used in Method-a, this method equally treats both substructures and dynamic integrations are performed in both

X and Y modules. This method is also known as the domain-decomposition method which is aimed to fully capture the dynamic interaction between different physical fields or domains. To distinct from Method-a, Method-b is referred to as the system-level decomposition method.
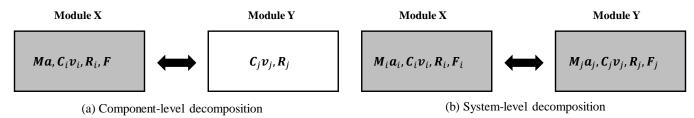
Module X

$$Ma, C_i v_i, R_i, F$$

Module Y

$$C_j v_j, R_j$$

Module X

$$M_i a_i, C_i v_i, R_i, F_i$$

Module Y

$$M_j a_j, C_j v_j, R_j, F_j$$

(a) Component-level decomposition

(b) System-level decomposition

Figure 1. Component-level vs. system-level decomposition

A generalized method to allow component-level decompositions has been developed by the authors [3]. This study only focuses on the development of system-level decomposition method which involves coupling of dynamic systems.

System-level decompositions are initiated from the domain decomposition methods which are used to solve coupled multiphysics problems, such as fluid-structure interaction and soil-structure interaction. The advent of parallel computing and hybrid simulations extend the method to analyze large-scale or complex systems by dividing the system into small problems which can be solved with different processors or with different approaches [4]. The decomposed subsystems can be solved using either monolithic or partitioned approaches. Based on the definitions in Felippa et al. [5], monolithic methods refer to the ones where the whole problem is treated as a monolithic entity, and all system components advanced simultaneously in time. Although the methods allow each subsystem to formulate its own equation, the response of each subdomain is obtained from the solution of a single governing equation of the entire system considering the contributions from all involved subsystems. Therefore, the interaction effects among the subsystems are directly taken into account. The monolithic methods are also referred to as direct or standard methods [6]. The partitioned methods, on the other hand, treat the problem as isolated entities that are separately stepped in time. The methods involve independent formulations as well as solutions of the governing equations of the subsystems. Therefore, different time integration schemes (or integrators) can be used. The interaction effects between the subsystems are considered by iteratively passing solution variables at the interface from one subsystem to the others until the convergence criterion is achieved [7]. The partitioned methods recently attracted more attention since it overcomes the implementation difficulties in the monolithic methods [8].
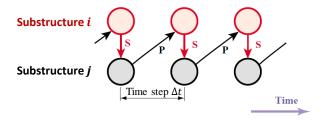
Substructure *i*

Substructure *j*

Time step Δ*t*

Time

Figure 2. Typical staggered solution approach for a two-field problem [5]

The partitioned algorithms can be implemented in a staggered or an iterative manner. In staggered methods, there are two analysis phases for each time step analysis: prediction (P) and substitution (S). As illustrated in Figure 2, each time step analysis starts from one of the substructures, substructure i, by introducing a predictor which can be displacement, velocity, acceleration, and force at the interface degrees of freedom (DOFs). Such predictor is then sent to the other substructure, substructure j. Once the substructure j is solved, the interface response is substituted into the substructure i such that a new predictor can be generated for the next time step analysis. The method is clearly approximate as most likely the boundary conditions at the interface obtained from the prediction and substitution phases are different. Such difference indicates a violation of either the compatibility or equilibrium condition at the interface, which in turn deteriorates stability and accuracy [9]. Generally, only conditional stability can be achieved when a staggered algorithm is used, and its performance is strongly dependent on the assumption made in the prediction phase. The iterative methods can be viewed as an improved version of the staggered methods to satisfy compatibility and equilibrium at the interface through corrective iterations. Although the iterative methods have been proven to be superior to the conventional staggered methods in accuracy and stability, they are more suited to be implemented in a single program as the methods involve rolling back the analysis for iterations [10–12]. Because iterations are not required, the staggered method is thus considered to be more ideal for reuse of existing code.

The objective of this study is to develop a system-level decomposition method to allow direct coupling of dynamic substructures modelled with different analysis programs. The method is aimed to have to the following features:

- Data exchange between the subsystems is only based on numerical model's standard input/output such that the implementation of the proposed method to existing analysis tools is straightforward. Each involved analysis program is treated as a black box and access to the source code is not necessary.
- Different from many other staggered partitioned methods whose stability characteristics are difficult to be evaluated, a stability proof is available to determine the maximum time step for stable solutions.

COUPLING METHODOLOGY

The system's equation of motion can be solved numerically using step-by-step integration schemes. Considering the widely used α-modified equation of motion in structural dynamics [13], a linear system can be expressed as

$$\boldsymbol{M}\boldsymbol{a}_{n+1} + (1+\alpha)\boldsymbol{C}\boldsymbol{v}_{n+1} - \alpha\boldsymbol{C}\boldsymbol{v}_n + (1+\alpha)\boldsymbol{R}(\boldsymbol{d}_{n+1}) - \alpha\boldsymbol{R}(\boldsymbol{d}_n) = (1+\alpha)\boldsymbol{F}_{n+1} - \alpha\boldsymbol{F}_n \tag{4}$$

where $\boldsymbol{R}(\boldsymbol{d}_{n+1})$ and $\boldsymbol{R}(\boldsymbol{d}_n)$ are restoring force with respect to $\boldsymbol{d}_{n+1}$ and $\boldsymbol{d}_n$, respectively, α is a coefficient allowing the tuning of the numerical damping to filter out undesired spurious high frequencies. A lower value of α, which is a negative term, leads to a larger numerical damping. The computations of displacement and velocity can be generalized to have a predictor step and a corrector step.

A predictor step:

$$\tilde{\boldsymbol{d}}_{n+1} = \boldsymbol{d}_n + \Delta t \boldsymbol{v}_n + \frac{1-2\beta}{2}\Delta t^2 \boldsymbol{a}_n \tag{5}$$

$$\tilde{\boldsymbol{v}}_{n+1} = \boldsymbol{v}_n + (1-\gamma)\Delta t \boldsymbol{a}_n \tag{6}$$

A corrector step:

$$\boldsymbol{d}_{n+1} = \tilde{\boldsymbol{d}}_{n+1} + \beta\Delta t^2 \boldsymbol{a}_{n+1} \tag{7}$$

$$\boldsymbol{v}_{n+1} = \tilde{\boldsymbol{v}}_{n+1} + \gamma\Delta t \boldsymbol{a}_{n+1} \tag{8}$$

where Δt is time increment, and β and γ are integration coefficients. With specific values of the coefficients, the derived integration scheme can be explicit or implicit. In the predictor step, the nodal displacements and velocities at the time step $n+1$ are explicitly obtained from the state values at the previous time step n. The predicted displacements and velocities are then corrected using the information, i.e. $\boldsymbol{a}_{n+1}$, at the current time step in the corrector step. Based on Eq. 5 to Eq. 8, Eq. 4 can be transformed into an effective equation as

$$\boldsymbol{A}\boldsymbol{a}_{n+1} = \boldsymbol{B}_{n+1} \tag{9}$$

with

$$\boldsymbol{A} = \boldsymbol{M} + (1+\alpha)\gamma\Delta t\boldsymbol{C} + (1+\alpha)\beta\Delta t^2\boldsymbol{K} \tag{10}$$

$$\boldsymbol{B}_{n+1} = (1+\alpha)\boldsymbol{F}_{n+1} - \alpha\boldsymbol{F}_n - (1+\alpha)\boldsymbol{C}\tilde{\boldsymbol{v}}_{n+1} + \alpha\boldsymbol{C}\boldsymbol{v}_n - (1+\alpha)\boldsymbol{R}(\tilde{\boldsymbol{d}}_{n+1}) + \alpha\boldsymbol{R}(\boldsymbol{d}_n) \tag{11}$$

A generalized form of the effective equation for the substructure i (sub-i) interfacing with the substructure j (sub-j) can be formulated as

$$(\boldsymbol{A}_i + \boldsymbol{A}_{ij})\boldsymbol{a}_{i,n+1} = \boldsymbol{B}_{i,n+1} + \boldsymbol{D}_{ij,n+1} \tag{12}$$

with

$$\boldsymbol{A}_i = \boldsymbol{M}_i + (1+\alpha_i)\gamma_i\Delta t\boldsymbol{C}_i + (1+\alpha_i)\beta_i\Delta t^2\boldsymbol{K}_i \tag{13}$$

$$\boldsymbol{B}_{i,n+1} = (1+\alpha_i)\boldsymbol{F}_{i,n+1} - \alpha_i\boldsymbol{F}_{i,n} - (1+\alpha_i)\boldsymbol{C}_i\tilde{\boldsymbol{v}}_{i,n+1} + \alpha_i\boldsymbol{C}_i\boldsymbol{v}_{i,n} - (1+\alpha_i)\boldsymbol{R}_i(\tilde{\boldsymbol{d}}_{i,n+1}) + \alpha_i\boldsymbol{R}_i(\boldsymbol{d}_{i,n}) \tag{14}$$

where subscripts i and j represent sub-i and sub-j, respectively. $\boldsymbol{A}_{ij}$ and $\boldsymbol{D}_{ij,n+1}$ represent the interaction terms that sub-j imposes to the sub-i. In this study, the interaction terms are approximated as below.

$$A_{ij} = \begin{pmatrix} 0 & 0 \\ 0 & M_j^B \end{pmatrix} \tag{15}$$

$$D_{ij,n+1} = \begin{pmatrix} 0 \\ (1 + \alpha_i)F_{j,n+1}^B - \alpha_i F_{j,n+1}^B - (1 + \alpha_i)\left(C_j^{BB}\tilde{v}_{j,n+1}^B + C_j^{BI}\tilde{v}_{j,n+1}^I\right) + \\ \alpha_i\left(C_j^{BB}v_{j,n}^B + C_j^{BI}v_{j,n}^I\right) - (1 + \alpha_i)R(\tilde{d}_{j,n+1}) + \\ \alpha_i R(\tilde{d}_{j,n}) \end{pmatrix} \tag{16}$$

where superscripts B and I are used to indicate the terms with respect to the DOFs at the interface boundary between sub-i and sub-j and the rest of the DOFs of sub-j, respectively.

The flow chart of the proposed method is given in Figure 3. The method is apparently staggered as the two substructures are alternatively integrated in time. Step 4 and step 7 in the figure correspond to the prediction and substitution phases in Figure 2, respectively. To distinguish the prediction and substitution phases in the proposed method, the substructure from which A_{ij} and $D_{ij,n+1}$ are predicted is referred to as a *primary* substructure (i.e. sub-j) while the other substructure which receives A_{ij} and $D_{ij,n+1}$ is referred to as a *secondary* substructure (i.e. sub-i). It is worth noting that the proposed method allows different numerical time integration schemes (i.e. different integration coefficients, α, β, and γ) to be used in the substructures.

1. Choose Δt
2. Sub-j predicts A_{ij} based on Eq. 15 and adds it to the interface boundary of Sub-i
3. Set $n = 0$
4. Sub-j predicts D_{ij} based on Eq. 16 and impose it to the interface boundary of Sub-i
5. Solve Sub-i for $a_{i,n+1}$ according to Eq. 12
6. Compute $d_{i,n+1}$ and $v_{i,n+1}$ of the Sub-i according to Eq. 7 and Eq. 8
7. Sub-i imposes $d_{i,n+1}^B$ to the interface boundary of the Sub-j.
8. Solve Sub-j according to Eq. 9
9. Set n = n+1 and go to step 4.

Figure 3. Time-stepping diagram of the proposed method

STABILITY ANALYSIS

The stability of the proposed method is evaluated in this section. Consider a mass-spring system which is decomposed into a *primary* substructure (sub-j) and a *secondary* substructure (sub-i) as shown in Figure 4 for example, step 7 in Figure 3 is equivalent to imposing an additional external load at the interface boundary of the *primary* substructure as shown in Figure 5(b). Since the sability of a numerical integration scheme is independent of the external load, the *primary* substructure has the same stability characteristics as its counterpart shown in Figure 5(d). In other words, the *primary* substructure is stable if the stability condition of the integration scheme used in its stability counterpart can be satisfied. Such stability counterpart can be obtained by fixing the interface DOFs of the *primary* substructure.
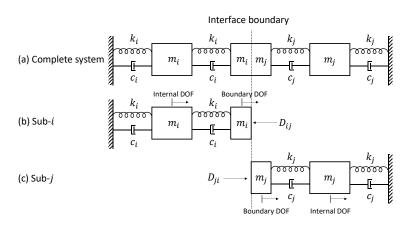
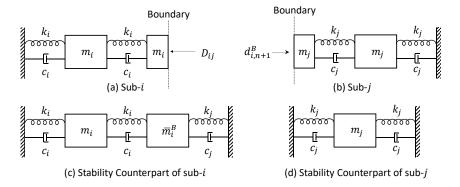*Figure 4. Example mass-spring system*

Figure 5. Stability counterparts of the primary and secondary substructures

For the *secondary* substructure in Figure 5(a), Eq. 12 can be expanded as

$$\overline{M}_i a_{i,n+1} + (1 + \alpha_i)\overline{C}_i v_{i,n+1} - \alpha_i \overline{C}_i v_{i,n} + (1 + \alpha_i)\overline{K}_i d_{i,n+1} - \alpha_i \overline{K}_i d_{i,n} = (1 + \alpha_i)\overline{F}_{i,n+1} - \alpha_i \overline{F}_{i,n} \tag{17}$$

where

$$\overline{M}_i = M_i + \begin{pmatrix} \mathbf{0} & \mathbf{0} \\ \mathbf{0} & M_j^B - (1 + \alpha_i)\gamma_i \Delta t C_j^{BB} - (1 + \alpha_i)\beta_i \Delta t^2 K_j^{BB} \end{pmatrix} \tag{18}$$

$$\overline{C}_i = C_i + \begin{pmatrix} \mathbf{0} & \mathbf{0} \\ \mathbf{0} & C_j^{BB} \end{pmatrix} \tag{19}$$

$$\overline{K}_i = K_i + \begin{pmatrix} \mathbf{0} & \mathbf{0} \\ \mathbf{0} & K_j^{BB} \end{pmatrix} \tag{20}$$

$$\overline{F}_{i,n+1} = F_{i,n+1} + \begin{pmatrix} \mathbf{0} \\ F_{j,n+1}^B - C_j^{BI}\widetilde{v}_{j,n+1}^I - K_j^{BI}\widetilde{d}_{j,n+1}^I \end{pmatrix} \tag{21}$$

$$\overline{F}_{i,n} = F_{i,n} + \begin{pmatrix} \mathbf{0} \\ F_{j,n}^B - C_j^{BI}v_{j,n}^I - K_j^{BI}d_{j,n}^I \end{pmatrix} \tag{22}$$

Eq. 17 describes a system with equivalent mass $\overline{M}_i$, equivalent damping $\overline{C}_i$, and equivalent stiffness $\overline{K}_i$. $\overline{F}_{i,n+1}$ and $\overline{F}_{i,n}$ are equivalent external forces which can be neglected for stability analysis. Such system has the same stability characteristics as the original *secondary* substructure. The system can be obtained by including the mass ($M_j^B - (1 + \alpha_i)\gamma_i \Delta t C_j^{BB} -$ $(1 + \alpha_i)\beta_i \Delta t^2 K_j^{BB}$), stiffness ($K_j^{BB}$) and damping ($C_j^{BB}$) of the *primary* substructure at the interface boundary to the *secondary* substructure. For example, the stability counterpart of the *secondary* substructure of the mass-spring system is shown in Figure 5(c). The equivalent mass $\overline{m}_i^B$ at the interface node equals to $m_i + m_j - (1 + \alpha_i)\gamma_i \Delta t c_j - (1 + \alpha_i)\beta_i \Delta t^2 k_j$. If $\overline{m}_i^B \geq 0$, the

known stability criterion of the integration scheme used in the stability counterpart can be used to determine the stability of the *secondary* substructure. For *secondary* substructures with multiple DOFs at the interface boundary, the equivalent interface mass is shown in Eq. 23 which should be positive definite.

$$\overline{\boldsymbol{M}}_i^B = \boldsymbol{M}_i^B + \boldsymbol{M}_j^B - (1 + \alpha_i)\gamma_i \Delta t \boldsymbol{C}_j^{BB} - (1 + \alpha_i)\beta_i \Delta t^2 \boldsymbol{K}_j^{BB} \tag{23}$$

Regardless of the integration schemes used in both *primary* and *secondary* substructures, the systems' stability based on the proposed method can be evaluated by following the steps below:

1. Define stability counterparts of *primary* and *secondary* substructures.

2. Find the critical time step $\Delta t_{cr,s}$ for each stability counterpart based on the known stability criterion of the numerical integration scheme used in the substructure s.

3. The time step Δt selected for the integrated simulation should satisfy

$$\Delta t \leq minmum(\Delta t_{cr,1}, \Delta t_{cr,2}, \ldots, \Delta t_{cr,h}) \tag{24}$$

where h is the total number of substructures.

In particular, if unconditionally stable integration schemes are used in both *primary* and *secondary* substructures, the stability of the integrated model based on the proposed method is solely dependent on the positive definiteness of the equivalent mass $\overline{\boldsymbol{M}}_i^B$ at interface boundaries of the *secondary* substructures.

IMPLEMENTATION

Based on a staggered scheme, the proposed method facilitates the reuse of existing FE codes for integrated simulations since only boundary quantities, i.e. $\boldsymbol{A}_{ij}$ and $\boldsymbol{D}_{ij,n+1}$, are required in the coupling process. As shown in Eq. 15, $\boldsymbol{A}_{ij}$ is the interface mass of the *primary* substructure. Since the mass does not change during the analysis in typical structural problems in civil engineering, it can be predefined once at the beginning of the analysis. The force $\boldsymbol{D}_{ij,n+1}$ shown in Eq. 16, on the other hand, includes predictors of damping and restoring forces which are difficult to acquire from an analysis program. However, if the *primary* substructure only includes thin layers of structural elements and they are assumed to be linear elastic, $\boldsymbol{D}_{ij,n+1}$ can be computed directly from Eq. 16 based on the predefined damping and stiffness matrices of the layers. For example, an integrated simulation of a gravity dam shown in Figure 6 can be decomposed into three *secondary* substructure models: the dam structure, the near-field soil domain, and the far-field soil domain. As shown in Figure 7, the decomposition of the system introduces two thin elastic layers of the soil elements modelled in a *primary* substructure model. Due to the small size of the layers compared to the *secondary* substructures, the error due to the assumption that the two layers are linear elastic is negligible.
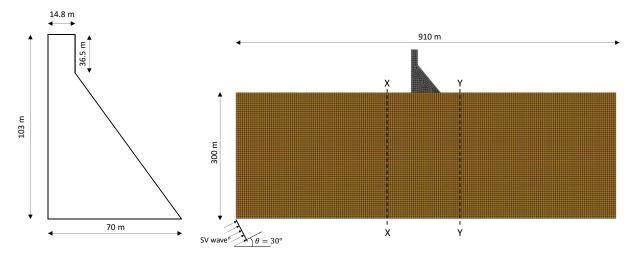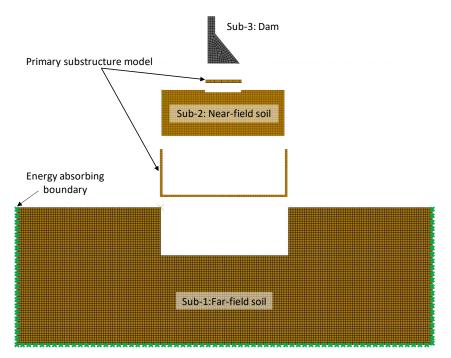

Figure 6. Geometry of a gravity dam system

Figure 7. Integrated model of the gravity dam system

APPLICATION EXAMPLE

The gravity dam system shown in Figure 6 was analyzed to demonstrate potential of the proposed method for integrated simulations of large structural systems. The dam had a height of 103 m and a width of 70 m. For the sake of simplicity, the dam was assumed to be linear elastic with an elastic modulus of 3.15×10^{10} N/m and a mass density of 2.42×10^3 kg/m^3. The dam was assumed to be built upon a hard rock soil with Young's modulus, mass density, and Poisson's ratio of 1.75×10^{10} N/m^2, 1.8×10^3 kg/m^3, and 0.2, respectively. The primary and shear wave velocities of hard rock were 3.28×10^3 m/s and 2.01×10^3 m/s. The system was assumed to be subjected to an incident shear wave as shown in Figure 6. The incident angle was 30° with respect to the horizontal axis. A Ricker wavelet with a maximum acceleration of 5.88 m/s^2 and a peak frequency of 1.5 Hz was used to represent the incident wave as shown in Figure 8.
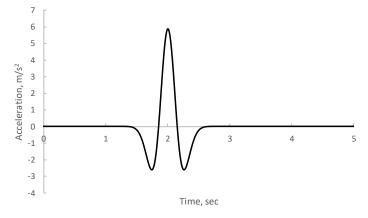

Figure 8. Incident motion time history

Figure 7 shows the decomposed substructures of the system, each of which was modelled with ABAQUS. Energy absorbing elements were used to mimic the infinite nature of the soil. The incident wave was applied in the far-field soil model as equivalent forces in the horizontal and vertical directions at the bottom boundary of the soil domain. Rayleigh's damping was used for the entire system with 5% damping specified in the first and second modes. The time step of the analysis was defined as 0.001 sec which was smaller than the critical time step based on the stability analysis method presented in this study.

The results of the integrated model were compared with those of the standalone model where the complete soil-dam system was modelled with ABAQUS. Figure 9 compared the two models in horizontal deflection histories at the two sections (i.e. X-

X and Y-Y) shown in Figure 6. The deflections predicted from the integrated model were in good agreement with those of the standalone model, which confirms the accuracy of the proposed method.
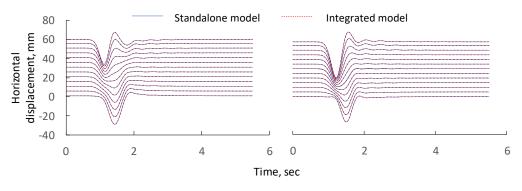

Figure 9. Predicted horizontal displacement histories of the sections X-X and Y-Y

SUMMARY

This paper presented a simulation method to integrate dynamic systems. The method used a staggered approach to allow data exchange only performed at the interface DOFs between the substructures thereby facilitating software reuse. The method is conditionally stable, and its stability can be evaluated through the stability analysis method developed in this study. Potential of the method for integrated simulations of large structural systems was demonstrated through an application example.

ACKNOWLEDGMENTS

REFERENCES

[1]   Hakuno, M., Shidawara, M., and Hara, T., 1969, "Dynamic Destructive Test of a Cantilever Beam Controlled by an Analog-Computer," Trans. Japan Soc. Civ. Eng., **1969**(171), pp. 1–9.

[2]   Takanashi, K., Udagawa, K., Seki, M., Okada, T., and Tanaka, H., 1975, *Nonlinear Earthquake Response Analysis of Structures by a Computer-Actuator on-Line System*, Bull. of Earthquake Resistant Structure Research Centre, No. 8, Institute of Industrial Science, University of Tokyo, Japan.

[3]   Huang, X., and Kwon, O. S., 2018, "A Generalized Numerical/Experimental Distributed Simulation Framework," J. Earthq. Eng., pp. 1–22.

[4]   Jia, C., 2010, "Monolithic and Partitioned Rosenbrock-Based Time Integration Methods for Dynamic Substructure Tests," Ph.D. Thesis, University of Trento.

[5]   Felippa, C. A., Park, K. C., and Farhat, C., 2001, "Partitioned Analysis of Coupled Systems," Comput. Methods Transient Anal., **190**, pp. 3247–3270.

[6]   Soares jr., D., and Godinho, L., 2014, "An Overview of Recent Advances in the Iterative Analysis of Coupled Models for Wave Propagation," J. Appl. Math., **2014**, pp. 1–21.

[7]   Rugonyi, S., and Bathe, K., 2001, "On Finite Element Analysis of Fluid Flows Fully Coupled with Structural Interactions," Comput. Model. Eng. Sci., **2**(2), pp. 195–212.

[8]   Harapin, A., Radnić, J., and Sunara, M., 2015, "Numerical Simulation of Coupled Problems," Comput. Methods Appl. Mech. Eng., **59**, pp. 121–133.

[9]   Giles, M. B., 1997, "Stability and Accuracy of Numerical Boundary Conditions in Aeroelastic Analysis," Int. J. Numer. Methods Fluids, **24**(8), pp. 739–757.

[10]   Gravouil, A., and Combescure, A., 2001, "Multi-Time-Step Explicit – Implicit Method for Non-Linear Structural Dynamics," Int. J. Numer. Methods Engin, **50**, pp. 199–225.

[11]   Gravouil, A., Combescure, A., and Brun, M., 2015, "Heterogeneous Asynchronous Time Integrators for Computational Structural Dynamics," Int. J. Numer. Methods Eng., **102**, pp. 202–232.

[12]   Pan, P., Tomofuji, H., Wang, T., Nakashima, M., Ohsaki, M., and Mosalam, K. M., 2006, "Further Remark on P Systems with Active Membranes and Two Polarizations," Earthq. Eng. Struct. Dyn., (35), pp. 867–890.